AMERICAN SOCIETY FOR MICROBIOLOGY | Antimicrobial Agents and Chemotherapy

Selective Inactivity of Pyrazinamide against Tuberculosis in C3HeB/FeJ Mice Is Best Explained by Neutral pH of Caseum

Jean-Philippe Lanoix,[a,b] Thomas Ioerger,[c] Aimee Ormond,[a] Firat Kaya,[d] James Sacchettini,[c] Véronique Dartois,[d] Eric Nuermberger[a,e]

Center for Tuberculosis Research, Department of Medicine, Johns Hopkins University School of Medicine, Baltimore, Maryland, USA[a]; INSERM U1088, Amiens, France[b]; Department of Computer Science, Texas A&M University, College Station, Texas, USA[c]; Public Health Research Institute and New Jersey Medical School, Rutgers, The State University of New Jersey, Newark, New Jersey, USA[d]; Department of International Health, Johns Hopkins Bloomberg School of Public Health, Baltimore, Maryland, USA[e]

Pyrazinamide (PZA) is one of only two sterilizing drugs in the first-line antituberculosis regimen. Its activity is strongly pH dependent; the MIC changes by several orders of magnitude over a range of pH values that may be encountered in various *in vivo* compartments. We recently reported selective inactivity of PZA in a subset of C3HeB/FeJ mice with large caseous lung lesions. In the present study, we evaluated whether such inactivity was explained by poor penetration of PZA into such lesions or selection of drug-resistant mutants. Despite demonstrating similar dose-proportional PZA exposures in plasma, epithelial lining fluid, and lung lesions, no dose response was observed in a subset of C3HeB/FeJ mice with the highest CFU burden. Although PZA-resistant mutants eventually replaced the susceptible bacilli in BALB/c mice and in C3HeB/FeJ mice with low total CFU burdens, they never exceeded 1% of the total population in nonresponding C3HeB/FeJ mice. The selective inactivity of PZA in large caseous lesions of C3HeB/FeJ mice is best explained by the neutral pH of liquefying caseum.

Pyrazinamide (PZA) is one of only two drugs proven to be capable of shortening the duration of treatment for tuberculosis (TB) to less than 12 months (1, 2). Although it has been a part of first-line treatment regimens for 40 years, its mechanism of action remains incompletely understood (3, 4). PZA is a prodrug that is converted to the active moiety pyrazinoic acid (POA) by a bacterial amidase encoded by *pncA* (3). The MICs of both PZA and POA against *Mycobacterium tuberculosis* are profoundly pH dependent, changing by several orders of magnitude over the range of pH values that may be encountered *in vivo*. For example, the PZA MIC is 1,000 μg/ml at a pH of 6.8, 50 μg/ml at a pH of 5.5, and theoretically as low as 5 μg/ml at a pH of 4.5, which *M. tuberculosis* may encounter in the phagolysosomes of activated macrophages (5–7). Thus, just as its activity *in vivo* is assumed to vary according to drug exposure at the site of infection, it also should vary significantly according to the pH at the site of infection.

The treatment-shortening, or sterilizing, effect of PZA in human TB is not readily evident in its early bactericidal activity (EBA), as measured by the average daily fall in the sputum CFU count over the first 14 days of treatment. The EBA of PZA monotherapy ranges from 0.04 to 0.1 $\log_{10}$ CFU/ml/day (8, 9). When administered in combination with isoniazid and rifampin, its contribution to the EBA of the regimen may be undetectable (8). Instead, the contribution of PZA is more evident during the later phase of sputum sterilization (8, 10). It is remarkable, then, that PZA exerts its treatment-shortening effect in the modern short-course regimen only during the first 2 months of treatment. Extending the duration of treatment has no additional benefit, in both humans and murine models (3, 11, 12).

Taken together, these characteristics suggest that PZA exerts its unique sterilizing effect against a subpopulation of tubercle bacilli residing in one or more specific compartments where the pH is sufficiently low to make the bacilli more susceptible to PZA than to other drugs. Where such subpopulations reside remains incompletely understood. It has been proposed that PZA acts against bacilli in inflammatory lung lesions, where the pH is presumed to be acidic (e.g., 5.5 to 6.0) initially and then to increase as the lesions resolve with effective treatment (13). Alternatively, the acidic milieu may persist but the bacillary subpopulation that resides in that milieu, making it more susceptible to PZA than to another first-line drug (e.g., rifampin), may simply be eradicated after 2 months of first-line therapy.

Active TB in humans is characterized by a variety of lesion types in which *M. tuberculosis* encounters different microenvironments. Although no single nonclinical model of TB recapitulates all aspects of human TB, existing models may be used in a complementary fashion to better understand the impact of the lesion type and resultant microenvironmental conditions on the action of PZA in human disease (14, 15). Based on pharmacodynamics (PD) studies in an *in vitro* hollow-fiber model of TB, Gumbo et al. proposed that PZA exerts its sterilizing effect against extracellular bacilli because PZA accumulates to concentrations high enough to produce its observed EBA at a pH of 5.8 only in alveolar epithelial lining fluid (ELF) (16), and not inside alveolar macrophages (17). However, there is no direct evidence that the ELF or the caseous material inhabited by extracellular *M. tuberculosis in vivo* is indeed this acidic. Moreover, PZA clearly exerts substantial bactericidal and sterilizing activities against established *M. tuberculosis* infection in BALB/c mice, where the infecting bacilli are virtually all intracellular. In fact, bactericidal activity is evident in BALB/c mice at doses producing plasma exposures approximately half

Received 12 June 2015 **Returned for modification** 23 August 2015
Accepted 8 November 2015
Accepted manuscript posted online 16 November 2015
Citation Lanoix J-P, Ioerger T, Ormond A, Kaya F, Sacchettini J, Dartois V, Nuermberger E. 2016. Selective inactivity of pyrazinamide against tuberculosis in C3HeB/FeJ mice is best explained by neutral pH of caseum. Antimicrob Agents Chemother 60:735–743. doi:10.1128/AAC.01370-15.
Address correspondence to Eric Nuermberger, enuermb@jhmi.edu.

those produced by standard human doses (e.g., 75 mg/kg of body weight in mice), both alone and in combination with rifampin and isoniazid (18). The pronounced effect of PZA in the intracellular compartment is presumably due to the more acidic milieu in the phagolysosomes of activated macrophages, where the pH can be as low as 4.5 (6, 7), making PZA capable of significant sterilizing effects. The key role of macrophage activation in optimizing the PZA effect is further supported by the poor activity of PZA in mice prior to the onset of the adaptive immune response and in athymic nude mice (19, 20).

C3HeB/FeJ mice have recently garnered significant attention as a murine TB model because, unlike BALB/c and other commonly used mouse strains, they develop caseous lung lesions in response to infection with *M. tuberculosis* (21–23). As expected, bacilli in the caseous cores of these lesions are extracellular, while the cellular cuffs of caseous granulomas and other nonnecrotic cellular granulomas harbor intracellular bacilli. Moreover, due to differences in the rate and extent of development of caseous lesions, significant heterogeneity in the presence, size, and degree of liquefaction of caseous lesions is often observed between mice and between lesions within the same mouse at the initiation of treatment. We recently described a surprising phenomenon of dichotomous activity of PZA in C3HeB/FeJ mice (24), where PZA had little or no detectable bactericidal activity in a subset of mice with large caseous lesions despite demonstrating the expected bactericidal effect in those with less extensive disease and in a parallel cohort of BALB/c mice. Based on this apparent lesion-dependent activity, we hypothesized that this dichotomous effect of PZA was due to its limited activity against extracellular bacilli in caseum, which comprise the majority population in C3HeB/FeJ mice with large caseous lesions, but bactericidal effects on the smaller numbers of bacilli in cellular lesions of BALB/c and C3HeB/FeJ mice and in the cellular cuffs of necrotic granulomas of C3HeB/FeJ mice. However, in C3HeB/FeJ mice with large caseous lesions, the effect against intracellular bacilli is largely obscured by the limited effect on the majority bacillary population in caseum.

In the present study, we set out to determine whether this selective inactivity of PZA in large caseous lesions could be explained by reduced drug penetration, selection of PZA-resistant mutants, or insufficiently acidic conditions for PZA activity at achievable PZA concentrations. The results indicate that the nearly neutral pH of liquefying caseum prevents PZA from exerting any significant bactericidal activity against the numerous extracellular bacilli in larger caseous lesions and support the concept that pronounced sterilizing effects of PZA are exerted against intracellular bacilli.

(Portions of the results of this study have been presented previously at the International Workshop on the Clinical Pharmacology of Tuberculosis Drugs [25], Washington, DC, September 2014, and the Interscience Conference on Antimicrobial Agents and Chemotherapy [26], Washington, DC, September 2014.)

MATERIALS AND METHODS

Mycobacterial strains. *M. tuberculosis* H37Rv was used as a frozen stock prepared from a log-phase culture in Middlebrook 7H9 broth after mouse passage and was diluted in 7H9 broth supplemented with 10% oleic acid-albumin-dextrose-catalase (OADC) before infection.

Drugs and chemotherapy. PZA was obtained from Acros Organics (Thermo Fisher Scientific, NJ) and formulated for oral administration in distilled water. The daily doses were 10, 30, 100, 150, 300, and 900 mg/kg of body weight. The most highly concentrated dosing solutions were warmed before administration to keep PZA in solution.

Doses were administered once daily 5 days/week by oral gavage, except for the 900-mg/kg dose, which was administered as 450 mg/kg twice daily (BID) due to solubility issues.

Mouse aerosol infection. All animal procedures were approved by the Animal Care and Use Committee of Johns Hopkins University. Female BALB/c mice (Charles River, Wilmington, MA) and C3HeB/FeJ mice (Jackson, Bar Harbor, ME) were used. The ages of the mice varied between 1.5 and 10 months.

Mice were aerosol infected using the Inhalation Exposure System (Glas-Col, Terre Haute, IN) with dilutions of a titered frozen stock of *M. tuberculosis* H37Rv to implant into the lung approximately 100 to 250 CFU for BALB/c mice and 50 to 100 CFU for C3HeB/FeJ mice. One day after infection, 4 mice from each aerosol run were humanely killed to determine the number of bacteria implanted.

Guinea pig aerosol infection. Female Hartley guinea pigs (Charles River, Wilmington, MA) 6 to 7 weeks old were aerosol infected with *M. tuberculosis* CDC1551 using a Madison chamber, as previously described (27).

Pharmacokinetic studies. Several pharmacokinetic (PK) studies were performed in C3HeB/FeJ mice to enable comparisons with results in BALB/c mice. The single-dose plasma and lung concentration-time profiles were determined in both 6- to 7-week-old and 8- to 10-month-old mice. Steady-state plasma and lung concentration-time profiles were determined in infected 5- to 10-month-old mice.

PZA concentrations were measured in samples of plasma, epithelial lining fluid (ELF), and lung lesions obtained, depending on the study, at 0.08, 0.25, 0.45, 1.5, 3, 5, 7, 12, and 17 h after PZA dosing. Three or four mice from each dose group were sampled at each time point. Plasma was obtained either by tail vein bleed or by cardiac puncture performed under anesthesia by isoflurane inhalation. ELF was obtained after centrifugation of bronchoalveolar lavage fluid (BALF) at 400 × *g* for 5 min. BALF was obtained, after anesthesia by intraperitoneal injection of ketamine (200 mg/kg) plus xylazine (10 mg/kg), by injection and aspiration of 300 μl of phosphate-buffered saline (PBS) via a 20-gauge (G) intravenous (i.v.) catheter (ProtectIV Plus; Smith Medical ASD, Southington, CT). The procedure was performed under visual control using an optic fiber (UV-visible [Vis] fiber; 0.22 numerical aperture [NA]; 400 μm; Edmund Optics, Barrington, NJ) and a fiberscope light source. Lung lesions were obtained by resecting single or coalescing tubercular lesions, minimizing the amount of normal-appearing lung resected, to obtain at least 20 mg of tissue. Lungs were rinsed in cold PBS, and lesions were resected on dry ice to prevent PZA diffusion or degradation.

Samples were frozen at −80°C before being shipped to the Dartois laboratory, Rutgers, NJ, Medical School, for quantification.

Quantification of PZA in samples. PZA standards were obtained from Acros Organics (Thermo Fisher Scientific, NJ). Analytes of interest were extracted by diluting 50 μl of mouse serum with 50 μl of acetonitrile-water (1:1) and 450 μl of methanol-acetonitrile (1:1) containing 0.5 μg/ml of pyrazinamide-^{15}N,d3 or pyrazinecarboxylic acid-d3 (Toronto Research Chemicals, Inc.) as an internal standard. The mixture was vortexed and centrifuged, and 200 μl of the supernatant was recovered for analysis. Liquid chromatography-tandem mass spectrometry (LC–MS-MS) analysis was performed with an Agilent 1260 system coupled to an AB Sciex 4000 Q-trap mass spectrometer (positive-mode electrospray ionization) and an Agilent column SB-C8 (4.6 by 75 mm; 3.5 μm), with the column temperature fixed at 24°C. Mobile phase A was 0.1% formic acid in 100% H_2O, and mobile phase B was 0.1% formic acid in 100% acetonitrile. Injection volumes were routinely 2 μl. The mass selective detector was set to MRM (multiple-reaction-monitoring) mode using positive polarity ionization, monitoring for the ions of interest (*m/z* 124.0/81.1 for PZA) and the internal standard (*m/z* 296/215). The lower limit of quantification was 0.2 μg/ml.

The urea method was used to correct for dilution of ELF by PBS in

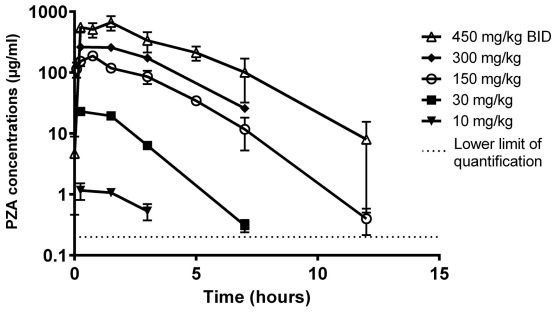

FIG 1 Dose-ranging PZA concentration-time profiles in uninfected C3HeB/FeJ mice in plasma. The data are plotted as means and SD.

BALF samples, as previously described (16). Thus, the concentration of PZA in ELF (Z_{ELF}) was derived from the following relationship: $Z_{ELF} = Z_{BAL} \times \{V_{BAL}/[V_{BAL} \times (U_{BAL}/U_{PLA})]\}$, where Z_{BAL} is the concentration of PZA measured in BALF, V_{BAL} is the volume of BALF, U_{BAL} is the concentration of urea in BALF, and U_{PLA} is the concentration of urea in plasma. Five microliters of plasma and 20 μl of ELF were used with the QuantiChrom urea assay kit (Gentaur, San Jose, CA), following the manufacturer's instructions.

PK parameters (area under the concentration-time curve [AUC_{0-t} or $AUC_{0-\infty}$], maximum concentration of drug in serum [C_{max}], and half-life [$T_{1/2}$]) were calculated from mean concentration data using Microsoft Excel (Office 2010; Microsoft Corp., Redmond, WA). The AUC was calculated using the linear trapezoidal rule. The half-life and elimination rate constant were calculated by linear regression using semilogarithmic concentration-versus-time data. Concentration values below the lower limit of quantification were excluded from the pharmacokinetic evaluation.

Pharmacodynamics study. To determine the dose-ranging efficacy of PZA, 60 BALB/c and 60 C3HeB/FeJ 6-week-old mice received 10, 30, 100, 300, and 450 mg/kg of PZA BID for up to 8 weeks, beginning 6 weeks after infection. Treatment efficacy was assessed on the basis of lung CFU counts determined after 3 and 8 weeks of treatment. Serial dilutions of whole lung homogenates were plated on selective Middlebrook 7H11 agar (Becton Dickinson, Franklin Lake, NJ). Plates were incubated for 6 to 8 weeks at 37°C before determining final CFU counts. At the 8-week time point, quantitative cultures were performed with 0.5 ml of lung homogenates on the same 7H11 agar supplemented with 900 mg/liter of PZA (which is 3 to 6 times the MIC against the parent H37Rv strain on this medium).

Whole-genome sequencing of PZA-resistant mutants. Genomic DNA extraction procedures were adapted from a previously described cetyltrimethyl ammonium bromide (CTAB)-lysozyme method (28). From 1 to 5 colonies per mouse were picked from PZA-containing plates and streaked on 7H11 agar to amplify the clone. Colonies were scraped and suspended by bead beating (2-mm sterile beads) in 5 ml of PBS. Three milliliters of supernatant was centrifuged for 2 min (3,340 × *g*) before the pellet was heat killed (30 min at 80°C) in 200 μl of Tris-EDTA (TE) buffer (Invitrogen, Gaithersburg, MD). After 5 min of centrifugation (3,340 × *g*), the pellet was incubated at 37°C overnight in 100 μl of lysozyme. The extract was incubated at 65°C twice for 10 min each time, once after addition of 20 μl of 5% sodium dodecyl sulfate (Bio-Rad, Hercules, CA) and 20 μl of 1-mg/ml proteinase K (Thermo Scientific, Waltham, MA) and once after addition of 20 μl of 3 M NaCl and 10 μl CTAB-NaCl solution. After adding chloroform-isoamyl alcohol (24:1 [vol/vol]), the solution was centrifuged for 8 min at 15,680 × *g*. The top layer was transferred into another tube containing 340 μl of ice-cold isopropanol before precipitating nucleic acids at −20°C for 30 min. After another centrifugation at 15,680 × *g* for 15 min, the pellet was washed with ice-cold 70% ethanol and then dissolved in 20 μl of pure water after a second centrifugation.

Samples were sequenced on an Illumina GAIIx next-generation sequencer. DNA samples were prepared for sequencing using the standard genomic-DNA sample preparation protocol (Illumina Inc., San Diego, CA). Paired-end data were collected, with a read length of 54 plus 54 bp. Base calling was performed using RTA 1.9.35 software (Illumina, San Diego, CA), and genome assembly was carried out using a comparative assembly technique, as described previously (29), using the genome of H37Rv as a reference sequence. The mean depth of coverage over all samples was 29.5×.

Assessment of the pH of the lesions. The pH of liquefied caseum from selected lesions of more than 3-mm diameter was measured with a 16-G needle tip micro-pH comb electrode (Thermo Scientific Orion, Chelmsford, MA) and a Mettler Toledo FE20 benchtop pH meter (Business Unit Analytical, Schwerzenbach, Switzerland). The probe was inserted directly into the tubercle to measure the pH of the liquefied material.

Data analysis. Lung CFU counts (x) were log transformed as $\log_{10}(x + 1)$ before analysis. Group mean CFU counts after 2 months of treatment were compared using one-way analysis of variance with GraphPad Prism v.5 (GraphPad Software, San Diego, CA) and Bonferroni's posttest to adjust for multiple comparisons, as appropriate. A nonlinear dose-response regression was used to calculate PZA dose response using the same software.

RESULTS

Pharmacokinetics of PZA. (i) Uninfected mice. Total daily doses of 10 to 900 mg/kg of PZA were administered. As stated in Materials and Methods, PZA was administered orally once a day, except for the 900-mg/kg dose, which was administered as two 450-mg/kg doses given 12 h apart (BID). PZA concentrations were measured in plasma and ELF.

As shown in Fig. 1, uninfected C3HeB/FeJ mice had at least dose-proportional (possibly supraproportional) exposures in plasma and also in ELF (data not shown). The PK parameter values for plasma are presented in Table 1 and were comparable to previously published results (30). The concentrations produced by the lowest doses of PZA were not quantifiable in ELF because of the high dilution factor. The median ELF/plasma concentration ratios ranged between 0.9 and 3 at 3 h and tended to increase slightly over time to 1.2 to 3.7 independently of the dose (except for the 300-mg/kg dose, where the ratio decreased) (Table 2).

(ii) Infected mice. Infected C3HeB/FeJ mice received 150-mg/kg once-daily or 450-mg/kg BID doses of PZA for 3 days or 4 weeks before PZA concentrations were measured in plasma, ELF, and tubercular lesions. No major difference was observed in

TABLE 1 Plasma PK parameters of PZA in C3HeB/FeJ mice[a]

Mice and infection status	PZA dose (mg/kg)	AUC_{0-24} (μg · h/ml)	C_{max} (μg/ml)	$T_{1/2}$ (h)
C3HeB/FeJ				
Uninfected (single dose)	10	9.2	5.6	0.6
	30	59.2	23	1
	150	577.9	187.8	1.4
	300	1,081.6	263	1.9
	450 BID	5,326.8	665.3	3.5
Infected (steady state)	150	455.6	166	1.3
	450 BID	3,589.6	467	1.6
BALB/c mice				
Infected (single dose)	150 (30)	388	163	1.2
	450 BID (unpublished data)	3,241.8	472.9	2.3

[a] Parameters were calculated from mean concentration data. The data presented are from one of two representative experiments for each infection condition.

TABLE 2 ELF/plasma PZA concentration ratios in C3HeB/FeJ mice

Mouse infection status	PZA dose (mg/kg)	Median ELF/plasma ratio (no. of mice) at[a]:			
		1.5 h	3 h	7 h	12 h
Uninfected (single dose)	30		1.2 (2)	3.7 (1)	
	150		0.9 (7)	1 (4)	22.8 (4)
	300		2 (6)	1 (5)	
	450 BID		1.1 (3)	2.2 (3)	1.2 (3)
Infected (steady state)	150	1.1 (6)	3 (7)	3.1 (8)	NA
	450 BID	1.3 (6)	1.6 (8)	1.2 (7)	

[a] NA, not applicable (due to a nonquantifiable PZA concentration in ELF or plasma). No PZA was measurable at 0-h and 17-h time points or in the 10-mg/kg arm.

plasma PZA concentrations between infected and uninfected mice, although AUC and C_{max} values were lower in infected mice receiving 450 mg/kg BID than in uninfected mice (Table 1). Plasma PK parameters in infected C3HeB/FeJ mice were comparable to past results in infected BALB/c mice (30) (Table 1). The dose proportionality was conserved both in plasma (Fig. 2) and in ELF. In ELF, PZA concentrations seemed to be more variable between mice and between experiments than what was observed in plasma (data not shown). The ELF/plasma PZA concentration ratio in infected mice was similar to that observed in uninfected mice (Table 2).

The concentrations of PZA in lesions largely mirrored the concentrations in plasma (Fig. 2). The measurements from a representative large necrotic granuloma sampled 7 h after a dose of 150 mg/kg were similar for the capsule and the liquefied caseum (2.68 and 1.76 μg/ml, respectively). When comparing PZA concentrations in lesions of mice with large necrotic granulomas (>3 mm) and mice without such lesions at the same time points, means tended to be higher in larger lesions than in smaller lesions. For example, in samples obtained 90 min after a 150-mg/kg dose, 3 large lesions had a mean PZA concentration of 105.1 μg/ml, whereas 3 smaller lesions averaged 80.1 μg/ml, but the difference was not statistically significant ($P = 0.07$). In samples obtained 7 h after the same dose, 3 large lesions had a mean PZA concentration of 3.5 μg/ml, whereas 2 smaller lesions averaged 2 μg/ml ($P = 0.055$). The median lesion/plasma concentration ratios were 0.8 and 0.7 at 1.5 h for 150 mg/kg and 450 mg/kg BID, respectively, and remained stable between 0.8 and 1.2 over time.

Pharmacodynamics of PZA. In the dose-ranging efficacy study, BALB/c and C3HeB/FeJ mice received daily doses ranging from 10 to 450 mg/kg of PZA BID for 3 to 8 weeks. Mean (standard deviation [SD]) CFU counts at the start of treatment (day zero [D0]) were 6.86 (0.17) for BALB/c mice and 7.09 (0.12) for C3HeB/FeJ mice. As previously described (24), PZA was associated with a dichotomous dose-response relationship in C3HeB/FeJ mice, but not in BALB/c mice. Dose-proportional bactericidal activity was observed in BALB/c mice and in most C3HeB/FeJ mice at each time point. At doses of 100 mg/kg and above, the size of the bactericidal effect increased between 3 and 8 weeks of treatment. After 8 weeks, increasing the dose from 30 to 300 mg/kg increased the log-kill by 2 $\log_{10}$ units, and increasing the dose from 300 mg/kg to 450 mg/kg BID increased the log-kill by another 2 $\log_{10}$ units in both mouse strains (Fig. 3). However, no dose-response effect was observed in a subset of C3HeB/FeJ mice, even after 8 weeks of treatment (Fig. 3). CFU counts after 8 weeks in these poor responders were 0.5 to 1 log unit lower than those at week 3, so some modest activity could not be excluded. Excluding these outliers, the goodness of fit of the logarithmic dose-response curves (r^2) was 0.92 at week 3 and 0.87 at week 8; the maximum effect (E_{max}) at week 3 was 3.27 $\log_{10}$, and the dose producing 50% of the E_{max} (50% effective concentration [EC_{50}]) was 128.4 mg/kg (95% confidence interval [CI] = 58.32 to 281.2). Similar curve fits and parameters were observed in BALB/c mice, e.g., the goodness of fit (r^2) was 0.87 and 0.98 at weeks 3 and 8, respectively; E_{max} was 3.06 $\log_{10}$; and the EC_{50} was 139.6 mg/kg (95% CI = 61.26 to 318.1) at week 3.

Selection and characterization of PZA-resistant mutants. After 8 weeks of treatment, 11 (37%) of 30 BALB/c mice had colonies on PZA-containing plates compared to 18 (75%) of 24 C3HeB/FeJ mice ($P < 0.01$). Resistance among BALB/c mice was observed only at PZA doses of ≥100 mg/kg, whereas resistance among C3HeB/FeJ mice was observed at all dose levels. Despite the proclivity for selection of resistant mutants in C3HeB/FeJ mice, replacement of the PZA-susceptible bacillary population with PZA-resistant mutants did not explain the poor activity of PZA in those with the highest CFU counts at the end of treatment. Indeed, the greatest proportion of PZA-resistant CFU compared to total CFU was among the C3HeB/FeJ mice receiving the highest PZA doses, in which the greatest bactericidal activity was observed (up to 100% of the total population was resistant to PZA). On the other

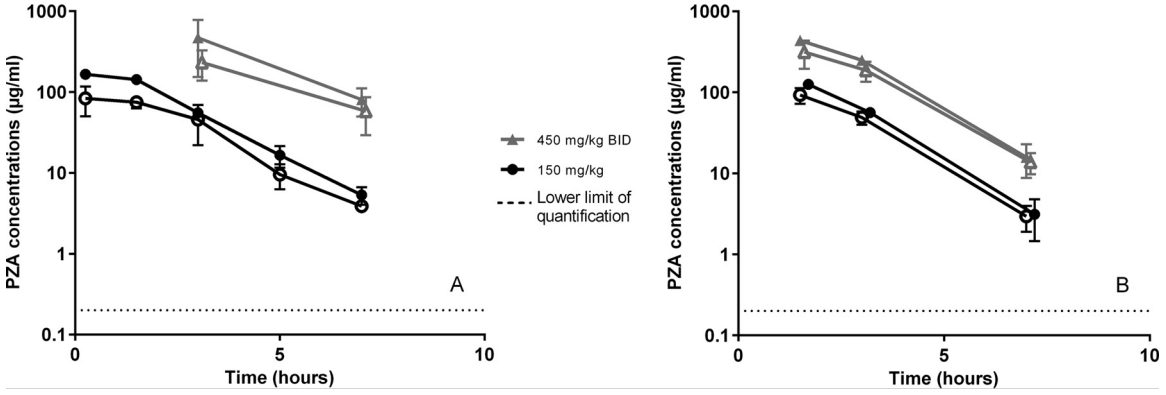

FIG 2 Dose-ranging PZA concentration-time profiles in infected C3HeB/FeJ mice in plasma (solid symbols) and lesions (open symbols) for doses of 150 and 450 mg/kg BID. Panels A and B represent 2 different sets of experiments. The data are plotted as means and SD.

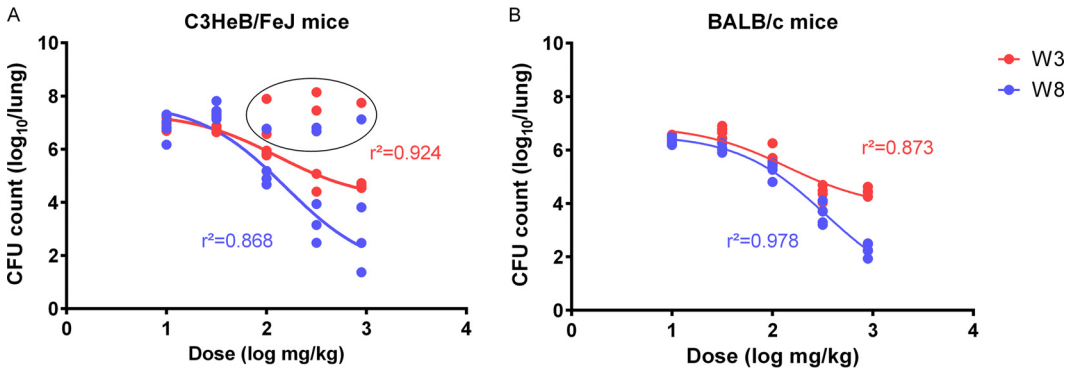

FIG 3 Dose-response profiles in C3HeB/FeJ mice (A) and BALB/c mice (B) after 3 weeks (blue) and 8 weeks (red) of treatment (W3 and W8, respectively). C3HeB/FeJ mice excluded from the curve fit (outliers) are circled.

hand, among mice in which PZA did not exhibit bactericidal activity, PZA-resistant mutants remained ≤1% of the total CFU (Fig. 4). Nevertheless, both the absolute number and the proportion of bacteria resistant to PZA tended to increase with the dose among the poorly responding C3HeB/FeJ mice, indicating that PZA was likely exerting a bactericidal effect against drug-susceptible bacilli and promoting selective amplification of resistant mutants within a minority subpopulation within these mice, likely in the intracellular compartment. The mean CFU counts of PZA-resistant mutants were not statistically different between the 2 mouse strains ($P = 0.89$, 0.11, and 0.17 for 100- and 300-mg/kg and 450-mg/kg BID doses, respectively).

Although colonies from each mouse harboring resistant mutants were processed for whole-genome sequencing, only 79% of the colonies selected (20/27 for BALB/c and 53/65 for C3HeB/FeJ mice) were actually sequenced due to a variety of technical difficulties.

With one exception, all sequenced colonies isolated on PZA-containing media had mutations in *pncA*, confirming the utility of employing 3× to 6× MIC PZA concentrations in standard 7H11 agar (pH 6.8) for isolating resistant mutants. In most cases, different colonies from the same mouse harbored the same *pncA* mutation. Out of 13 C3HeB/FeJ mice with several colonies sequenced, 2 mice had 3 or more colonies with differing mutations in *pncA*, whereas 7 mice had 2 colonies with either of 2 different mutations and 4 mice had colonies sharing only 1 mutation. Among 5 BALB/c mice with several colonies sequenced, 2 mice had colonies with either of 2 different *pncA* mutations and 3 mice had colonies sharing only 1 mutation. Table 3 catalogs the mutations identified, most of which have previously been reported as

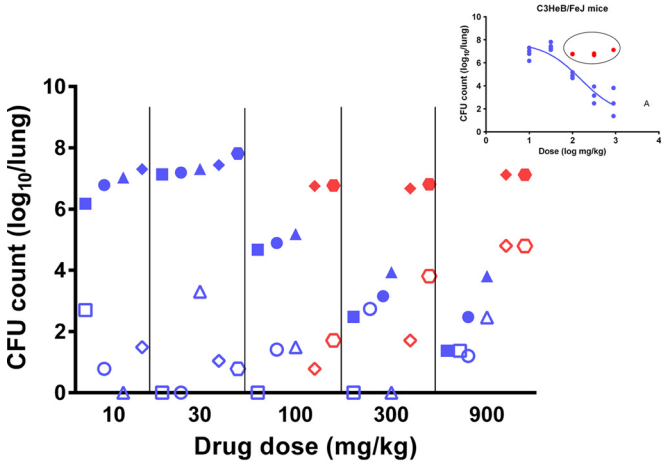

FIG 4 Total CFU counts (solid symbols) and PZA-resistant CFU counts (open symbols) in C3HeB/FeJ mice treated with increasing PZA doses. Each symbol shape represents an individual mouse in its dose group. Blue, CFU counts from mice considered to fit the dose-response curve shown in the inset; red, CFU counts from mice considered nonresponsive to the dose increase; solid symbols, total CFU counts determined on drug-free medium for each individual mouse; open symbols, resistant-CFU counts determined on PZA-containing plates for the same mouse.

TABLE 3 Results of mutations in the *pncA* gene (Rv2043c) observed in PZA-resistant isolates

Type of mutation	Mutation(s) in mouse strain:	
	BALB/c	C3HeB/FeJ
Point mutations	K96 M	M1I, T135P
	G132A	L19R, H137D
	C138Y	A46E, V139 M
	T142P	S67P, A146V
	L159V	H71Y, S164P
	H171R	C72F, L172P
		Y99stop, E173stop
		G108R
		I133N
Small indels[a]	+A in E127	−G in P54
		−CG in A26
		−T in I133
		−CGTCAGCGGTACTC in V73–P77
Large-scale deletions	Rv2023c–Rv2048c (27 kb)	Rv2030c–Rv2048c (21 kb)
	Rv2027c–Rv2047c (19.8 kb)	Rv2034–Rv2045c (9 kb)
		Rv2039c–Rv2048c (13 kb)
		Rv2040c–Rv2045c (3.5 kb)
		Rv2041c–Rv2043c (1.1 kb)
		Rv2042c–Rv2043c (1 kb)
		Rv2043c–Rv2044c (0.2 kb)
5′ UTR[b]	A→G at −11 bp (upstream)	
No *pncA* mutation		One (A3311T mutation in Rv3350c)

[a] Frameshifts.
[b] UTR, untranslated region.

clinically relevant mutations likely to confer PZA resistance (31; http://www.tbdreamdb.com/PZA_Rv2043c_AllMutations.html). Notably, deletions spanning multiple open reading frames were quite frequent (8/29 for C3HeB/FeJ versus 2/10 for BALB/c mice). Apart from deletions, seven different mutations in *pncA* were identified in BALB/c mice and 20 in C3HeB/FeJ mice. Each *pncA* mutation was observed in only one mouse. The only colony without a *pncA* mutation was selected in a C3HeB/FeJ mouse treated with a dose of 300 mg/kg and harbored only an A3311T mutation in Rv3350c (PPE56). Three other colonies isolated from the same mouse had this mutation, as well as identical 2-bp deletions in *pncA*. The fifth colony had no mutation in Rv3350c, only a different (G108R) mutation in *pncA*.

pH assessment. We recently reported that the pH of liquefied caseous material from lesions in C3HeB/FeJ mice was 7.39 ± 0.096 (range, 7.19 to 7.54) (24). To extend our evaluation to another nonclinical species, we measured pH values in 12 different lesions in 4 untreated guinea pigs infected for 13 weeks. An average pH of 7.23 ± 0.17 (range, 6.99 to 7.52) was found, only slightly lower than that of the adjacent normal-appearing lung (7.35 ± 0.22).

DISCUSSION

In a previous study, we observed that PZA had limited activity in a subset of C3HeB/FeJ mice with large caseous lesions and hypothesized that this was due to the neutral pH of the liquefied caseum in such lesions (24). In this study, we brought additional evidence in support of this hypothesis by demonstrating that neither poor distribution of PZA into caseous lesions nor selection of PZA-resistant mutants explains the limited PZA activity and the observed lack of dose-response effect.

Indeed PZA exposures increased in a dose-proportional fashion in plasma and ELF in both uninfected and infected mice and, at doses of 100 mg/kg or higher, met or exceeded plasma exposures observed in humans receiving PZA at doses recommended for TB treatment (16, 32). Moreover, PZA concentrations in the caseous lesions of infected C3HeB/FeJ mice also increased dose proportionally and were, on average, 67% of the concurrent plasma concentration, a ratio similar to that recently observed in a rabbit TB model and consistent with evidence that PZA diffuses readily through caseum (33–35). To our knowledge, this is the first report of PZA concentrations in ELF in mice. Conte et al. (16) described higher concentrations of PZA in ELF relative to plasma in uninfected human subjects (an ELF/plasma concentration ratio of 13 to 24) than we observed in infected mice, except for the median ratio of 22.8 we observed in mice sampled 12 h after a 150-mg/kg dose. This discrepancy may be due in part to the higher systemic clearance of PZA in mice, allowing less accumulation in ELF than in humans. However, determination of concentrations in ELF of rapidly diffusing small molecules like PZA is also technically challenging, because small differences in dwell time during bronchoalveolar lavage can introduce large differences in the concentration due to rapid drug redistribution from tissue into the lavage fluid (36). If the drug in question distributes more quickly than urea, its concentration in ELF could be overestimated as the dwell time of the lavage fluid increases. Importantly, infection did not appear to increase the distribution of PZA into the ELF.

As indicated by the lack of a dose-response effect in C3HeB/FeJ mice with large caseous lesions, achieving higher PZA concentrations is useful only if the pH of the actual lung compartment inhabited by *M. tuberculosis* is sufficiently acidic for PZA to exert its effect. According to the model of Zhang and Mitchison, intrabacillary accumulation of the active POA moiety increases inversely with the pH of the milieu (3). At neutral pH, the PZA MIC against *M. tuberculosis* H37Rv may exceed 1,600 μg/ml (5), which is 3 to 4 times higher than the highest average steady-state ELF concentrations observed in uninfected mice in this study or at 4 h postdose in uninfected human subjects administered 1 g daily for 5 days (16), as well as in infected mice receiving a PZA dose (150 mg/kg) that most closely approximates plasma AUCs observed in patients receiving recommended PZA doses. Only the C_{max} in the ELF of infected mice receiving 450 mg/kg BID approached the MIC at neutral pH.

Against cultures of *M. tuberculosis* H37Rv adjusted to a pH of 5.8 in an *in vitro* hollow-fiber model of TB, Gumbo et al. established that human-like exposures producing a PZA AUC of approximately 1,500 μg · h/ml (i.e., an AUC/MIC ratio of 120 multiplied by the MIC of 12.5) produces the same 0.11 $\log_{10}$ CFU/ml/day fall in CFU counts that was observed in 14-day clinical EBA trials (8, 17). Although the typical plasma AUC produced by standard PZA doses is only 300 to 500 μg · h/ml, the degree to which PZA was shown to accumulate in ELF provided a parsimonious explanation for sufficient target attainment in lung cavities, leading the authors to conclude that, because PZA does not accumulate above plasma concentrations inside cells, PZA most likely exerts its sterilizing activity against extracellular bacilli. However, the bactericidal and sterilizing activities of doses producing clinically relevant plasma PZA AUC values in commonly used mouse strains, in which virtually all bacilli are found intracellularly, are well demonstrated (11, 18, 37). In the present study, we found that after 15 doses of PZA administered to BALB/c mice, the EC_{50} of approximately 150 mg/kg produced a 0.102 $\log_{10}$ CFU/dose reduction. The mean plasma AUC produced by this dose is 388 μg · h/ml. Thus, a dose producing similar plasma AUC in BALB/c mice and humans produces similar EBA at exposures that are approximately one-quarter of the exposure required for the same effect in the hollow-fiber system at a pH of 5.8. The lower exposures needed to observe the same kill in mice as in the hollow-fiber system would be explained if the pH in infected murine macrophages is closer to 5.0, a level that is attained by activated macrophages (7, 38).

If extracellular bacilli are a target of PZA's sterilizing activity, then the pH of the ELF or caseum in which they are found should be sufficiently low for the expected PZA concentrations to be active. For example, a pH of 5.8 was studied in the hollow-fiber model (17). The technique of sampling ELF via BALF makes it difficult to measure the ELF pH. However, it is possible to measure the pH of airway lining fluid *in vivo*. The pH of the tracheal lining fluid of anesthetized mice was reported to be 7.1 (39). Similarly, a study using a bronchoscopically directed pH electrode reported the pH of subsegmental bronchi to be 6.6 in humans (6.48 in patients presenting with bacterial pneumonia) (40). Our finding of a more neutral pH in caseum from C3HeB/FeJ mouse and guinea pig tubercles extends previous work in rabbits showing an increase in the pH of caseum (from 6.4 to 7.4) as lesions mature, caseate, and liquefy (41). We are aware of only one report of the pH of caseum from human cavities, which described the pH of resected cavity tissue homogenates as ranging between 6.1 and 7.4 but noted that the pH was 6.8 or above in 15 out of 17 lesions (42). This report is well in line with the above-mentioned results from animal models. Taken together, these data run counter to the prevailing notion that caseum is acidic and make the assumption that

extracellular bacilli routinely encounter conditions where the pH is ≤6.5 rather tenuous (17).

The remarkable dichotomous activity of PZA in C3HeB/FeJ mice in the present study confirms and extends our prior results (24). It is also consistent with the important role of pH in the action of PZA. Among the mice with less severe disease, the pharmacodynamics of PZA were similar to those observed in BALB/c mice, suggesting similar conditions wherever bacilli are found intracellularly in C3HeB/FeJ mice, such as in small cellular granulomas or in the cellular cuffs of caseous granulomas. Based on the exposure-response relationship defined in the hollow-fiber model (17), the PZA exposures attained inside mouse macrophages would not be expected to exert a bactericidal effect comparable to the EBA in humans unless the pH in the macrophage compartment was below 5.8 and closer to 5.0, a value attainable in activated macrophages (7). On the other hand, in C3HeB/FeJ mice with large caseous lesions, where the pH approaches 7.4 (24), little or no bactericidal activity of PZA was observed, despite attaining plasma AUCs that are 3 to 5 times those produced in plasma at typical human doses but similar to the AUC associated with a 0.11 $\log_{10}$ CFU reduction per day at pH 5.8 in the hollow-fiber experiments (17). Moreover, the estimated PZA AUC in these lesions of approximately 850 μg · h/ml is the same as that associated with a 2-log-unit kill over 28 days in the hollow-fiber experiments. Taken together, these results are consistent with the idea that the local pH has a profound effect on PZA activity.

The facts that PZA exerts its sterilizing contribution during the first 2 months of treatment in the current first-line regimen and that patients unable to take PZA can still be cured when rifampin-containing regimens are given for 9 months rather than the usual 6 months with PZA (43) suggest that the bacillary population eradicated by PZA is not susceptible only to PZA, just more susceptible to PZA than to rifampin, and that this population is limited in size. When the pH is 6.5 and above, it is unlikely that PZA exposures routinely achieved in TB patients will produce the kind of bactericidal effect that will lend significant additive sterilizing activity to the first-line regimen. The high pH of the caseum lining the cavity wall likely explains the limited contribution of PZA to the activity of the first-line regimen over the first 14 days of treatment. There is ample evidence, however, that PZA contributes to the sterilization of sputum cultures later in the initial phase in patients receiving the first-line regimen, including recent evidence that this contribution is exposure dependent (10). While the poor results in mice with large caseous lesions seems inconsistent with the well-known treatment-shortening potential of PZA in humans, the results may be quite consistent if one considers that its sterilizing activity is evident only in the context of combination therapy. Our results suggest that, while other drugs, like rifampin and isoniazid, eradicate the bacilli in caseous material, PZA eliminates a subpopulation that likely resides inside macrophages, in phagolysosomes at low pH, where achievable PZA concentrations exceed the local MIC. The pH dependence of PZA activity, the nearly neutral pH of caseum across species, and the dramatic lesion dependence of PZA activity in C3HeB/FeJ mice provide compelling evidence that PZA exerts its most prominent sterilizing effects against intracellular bacilli. This model is not mutually exclusive with the model proposed by Gumbo et al., in which PZA exerts activity against extracellular bacilli in sufficiently acidic environments. Rather, given the remarkable heterogeneity observed in human TB, the models might be considered complementary. Further studies to evaluate the sterilizing activity of PZA in combination therapy and to isolate the lesions in C3HeB/FeJ mice in which PZA exerts a sterilizing effect are warranted.

We found that, like C3HeB/FeJ mice and rabbits, guinea pigs develop necrotic lesions with neutral caseum by 13 weeks postinfection. Despite this, PZA has been reported to have bactericidal activity in guinea pigs (37). This apparent discrepancy may be explained by the fact that examinations of lung histopathology revealed only poorly formed granulomas and limited necrosis at the time of treatment initiation (4 weeks postinfection) and active doses of PZA were associated with reduced numbers and size of granulomas (at 8 weeks postinfection) (37). Thus, it is likely that PZA exerted its bactericidal effect against bacilli under low-pH conditions inside activated macrophages rather than inside caseous regions. Further studies of PZA activity against more established disease in guinea pigs are warranted to test this hypothesis.

PZA resistance was not the explanation for the dichotomous activity of PZA in C3HeB/FeJ mice, since resistant mutants never replaced the sensitive population in the mice with the worst response to PZA. However, it is interesting that selective amplification of PZA-resistant mutants occurs more readily, including at lower doses, in C3HeB/FeJ mice than in BALB/c mice (18/24 versus 11/30, respectively). Many C3HeB/FeJ mice receiving doses of ≥100 mg/kg for 8 weeks harbored more than 0.1% PZA-resistant CFU, including mice in which the week 8 CFU count was likely not significantly lower than the D0 CFU count. This is evidence that, even when PZA was not exerting bactericidal effects on the largest population of bacilli in the large caseous lesions, it was exerting significant bactericidal activity against PZA-susceptible bacilli and selectively amplifying PZA-resistant mutants in smaller granulomas and cellular lesions similar to those in BALB/c mice. The limited effect of PZA in liquefied caseum, where the highest bacterial counts are observed, may help to explain why PZA resistance typically emerges only after resistance to rifampin and isoniazid and why PZA is not very effective at preventing the emergence of resistance to these and other companion agents that are bactericidal in that compartment (44). However, additional experiments comparing the selection of mutants resistant to PZA and to companion agents in large caseous lesions versus the rest of the lung are needed to confirm these results.

PZA resistance was explained by *pncA* mutations in all mice. Virtually all of these mutations have been described in PZA-resistant clinical isolates, and most of them were found only in PZA-resistant isolates, adding to the evidence presented here that these mutations confer PZA resistance (31). Therefore, C3HeB/FeJ mice may be an excellent model to study factors associated with the selection of PZA-resistant mutants and the clinical significance of specific mutations. It is noteworthy that large multigenic deletions, including *pncA* were observed in some PZA-resistant isolates from mice. Multigenic deletions are rare among reported clinical isolates (45, 46). However, they may be more difficult to detect by selective sequencing approaches commonly used with clinical isolates.

Our study has important limitations. First, we did not plate large caseous lesions in C3HeB/FeJ mice separately from the rest

of the lung, which prevented specific confirmation of where the selective killing of PZA-susceptible bacteria and amplification of PZA-resistant mutants were occurring. Second, in extrapolating the pH of TB lesion compartments from mice and other animal models to humans, we are limited by the scant data available on the pH of human caseum and the intracellular compartments inhabited by phagocytosed bacteria *in vivo*. Although further confirmation of the pH of human caseum is needed, the available data presented above suggest similar pH values across species. Although there is evidence that macrophages activated with interferon gamma *in vitro* deliver *M. tuberculosis* to an acidic compartment with a pH as low as 4.5 to 5.0 (7), confirmation of delivery of *M. tuberculosis* to acidified phagosomes in a living infected host was elusive until recently (47). Still, new tools are needed to more accurately quantify the pH of intracellular vacuoles and other lesion compartments inhabited by *M. tuberculosis in vivo* in a manner that can be correlated with PZA pharmacodynamics. A third limitation is that, due to the more rapid clearance of PZA in mice than in humans, the concentration-time profiles produced in our mice reproduced human AUCs but did not necessarily mimic the time course of PZA concentrations in humans. As mentioned above, this may be one reason for less accumulation of PZA in ELF of mice than in that of humans. It also may lead to discordance between the relationships of important PK/PD-based exposure indices and targets to efficacy and therefore demands caution when extrapolating between mice and humans or the hollow-fiber model, as we have here. A final limitation of this study is the high level of dilution (median = 1:40; interquartile range [IQR] = 1:21 to 1:64) of ELF with PBS, which made the lower limit of PZA quantification higher than that of plasma. The technical limit of quantification in each sample was 0.2 μg/ml, making the lower limit of quantification in ELF 4 to 13 μg/ml. Furthermore, BAL was performed with 300 μl of PBS, rendering it infeasible to duplicate samples or to repeat runs when results were not within 20% of controls (1 case out of 11).

Conclusions. In this study, we confirm that PZA has variable, lesion-dependent activity in C3HeB/FeJ mice in which poor PZA activity occurs in large caseous lesions due to the neutral pH of the caseum therein. Such lesion-dependent activity of PZA in C3HeB/FeJ mice, like that recently demonstrated for clofazimine and oxazolidinones (24, 48), promotes the C3HeB/FeJ mouse model as a valuable tool for studying the influence of the lesion type and the microenvironment on drug distribution and drug action, including the selection of drug-resistant mutants. Although additional studies to evaluate the contribution of PZA to the standard first-line regimen in C3HeB/FeJ mice are warranted, these results suggest that future investigations in C3HeB/FeJ mice may give a more holistic and nuanced appraisal of the potential contribution of PZA to novel regimens.

ACKNOWLEDGMENTS

This work has been funded by grants from the Bill and Melinda Gates Foundation (OPP1037174 [E.N.] and OPP1066499 [V.D.]) and a supplement to the Johns Hopkins University Center for AIDS Research (P30AI094189).

We thank Si-Yang Li, Jin Lee, and Fabrice Betoudji for their help during the experiments and Alvaro Ordonez and Bappaditya Dey for providing the interspecies animals. We also thank Anne Lenaerts, Khisi Mdluli, and Omar Vandal for valuable discussions of the results presented here and of the potential role of C3HeB/FeJ mice in preclinical drug development.

FUNDING INFORMATION

Bill and Melinda Gates Foundation provided funding to Eric Nuermberger under grant number OPP1037174. Bill and Melinda Gates Foundation provided funding to Veronique Dartois under grant number OPP1066499. National Institutes of Health (NIH) provided funding to Eric Nuermberger under grant number P30AI094189.

REFERENCES

1. **British Thoracic and Tuberculosis Association.** 1976. Short-course chemotherapy in pulmonary tuberculosis. A controlled trial by the British Thoracic and Tuberculosis Association. Lancet **ii:**1102–1104.
2. **British Thoracic Society.** 1984. A controlled trial of 6 months' chemotherapy in pulmonary tuberculosis. Final report: results during the 36 months after the end of chemotherapy and beyond. Br J Dis Chest **78:**330–336.
3. **Zhang Y, Mitchison D.** 2003. The curious characteristics of pyrazinamide: a review. Int J Tuberc Lung Dis **7:**6–21.
4. **Shi W, Zhang X, Jiang X, Yuan H, Lee JS, Barry CE, Wang H, Zhang W, Zhang Y.** 2011. Pyrazinamide inhibits trans-translation in Mycobacterium tuberculosis. Science **333:**1630–1632. http://dx.doi.org/10.1126/science.1208813.
5. **Zhang Y, Permar S, Sun Z.** 2002. Conditions that may affect the results of susceptibility testing of Mycobacterium tuberculosis to pyrazinamide. J Med Microbiol **51:**42–49. http://dx.doi.org/10.1099/0022-1317-51-1-42.
6. **Vandal OH, Pierini LM, Schnappinger D, Nathan CF, Ehrt S.** 2008. A membrane protein preserves intrabacterial pH in intraphagosomal Mycobacterium tuberculosis. Nat Med **14:**849–854. http://dx.doi.org/10.1038/nm.1795.
7. **MacMicking JD, Taylor GA, McKinney JD.** 2003. Immune control of tuberculosis by IFN-gamma-inducible LRG-47. Science **302:**654–659. http://dx.doi.org/10.1126/science.1088063.
8. **Jindani A, Doré CJ, Mitchison DA.** 2003. Bactericidal and sterilizing activities of antituberculosis drugs during the first 14 days. Am J Respir Crit Care Med **167:**1348–1354. http://dx.doi.org/10.1164/rccm.200210-1125OC.
9. **Diacon AH, Dawson R, von Groote-Bidlingmaier F, Symons G, Venter A, Donald PR, van Niekerk C, Everitt D, Hutchings J, Burger DA, Schall R, Mendel CM.** 2015. Bactericidal activity of pyrazinamide and clofazimine alone and in combinations with pretomanid and bedaquiline. Am J Respir Crit Care Med **191:**943–953. http://dx.doi.org/10.1164/rccm.201410-1801OC.
10. **Chigutsa E, Pasipanodya JG, Visser ME, van Helden PD, Smith PJ, Sirgel FA, Gumbo T, McIlleron H.** 2015. Impact of nonlinear interactions of pharmacokinetics and MICs on sputum bacillary kill rates as a marker of sterilizing effect in tuberculosis. Antimicrob Agents Chemother **59:**38–45. http://dx.doi.org/10.1128/AAC.03931-14.
11. **Grosset J, Truffot C, Fermanian J, Lecoeur H.** 1982. Sterilizing activity of the main drugs on the mouse experimental tuberculosis. Pathol Biol (Paris) **30:**444–448.
12. **Hong Kong Chest Service/British Medical Research Council.** 1991. Controlled trial of 2, 4, and 6 months of pyrazinamide in 6-month, three-times-weekly regimens for smear-positive pulmonary tuberculosis, including an assessment of a combined preparation of isoniazid, rifampin, and pyrazinamide. Results at 30 months. Hong Kong Chest Service/British Medical Research Council. Am Rev Respir Dis **143:**700–706.
13. **Mitchison DA, Fourie PB.** 2010. The near future: improving the activity of rifamycins and pyrazinamide. Tuberculosis **90:**177–181. http://dx.doi.org/10.1016/j.tube.2010.03.005.
14. **Gumbo T, Lenaerts AJ, Hanna D, Romero K, Nuermberger E.** 2015. Nonclinical models for antituberculosis drug development: a landscape analysis. J Infect Dis **211**(Suppl 3)**:**S83–S95. http://dx.doi.org/10.1093/infdis/jiv183.
15. **Lenaerts A, Barry CE, Dartois V.** 2015. Heterogeneity in tuberculosis pathology, microenvironments and therapeutic responses. Immunol Rev **264:**288–307. http://dx.doi.org/10.1111/imr.12252.
16. **Conte JE, Golden JA, Duncan S, McKenna E, Zurlinden E.** 1999. Intrapulmonary concentrations of pyrazinamide. Antimicrob Agents Chemother **43:**1329–1333.
17. **Gumbo T, Dona CS, Meek C, Leff R.** 2009. Pharmacokinetics-pharmacodynamics of pyrazinamide in a novel in vitro model of tuberculosis for sterilizing effect: a paradigm for faster assessment of new antitu-

berculosis drugs. Antimicrob Agents Chemother **53:**3197–3204. http://dx.doi.org/10.1128/AAC.01681-08.
18. **Ahmad Z, Tyagi S, Minkowsk A, Almeida D, Nuermberger EL, Peck KM, Welch JT, Baughn AS, Jacobs WR, Grosset JH.** 2012. Activity of 5-chloro-pyrazinamide in mice infected with Mycobacterium tuberculosis or Mycobacterium bovis. Indian J Med Res **136:**808–814.
19. **Almeida DV, Tyagi S, Li S, Wallengren K, Pym AS, Ammerman NC, Bishai WR, Grosset JH.** 2014. Revisiting anti-tuberculosis activity of pyrazinamide in mice. Mycobact Dis **4:**145.
20. **Rullas J, García JI, Beltrán M, Cardona PJ, Cáceres N, García-Bustos JF, Angulo-Barturen I.** 2010. Fast standardized therapeutic-efficacy assay for drug discovery against tuberculosis. Antimicrob Agents Chemother **54:**2262–2264. http://dx.doi.org/10.1128/AAC.01423-09.
21. **Davis SL, Nuermberger EL, Um PK, Vidal C, Jedynak B, Pomper MG, Bishai WR, Jain SK.** 2009. Noninvasive pulmonary [18F]-2-fluoro-deoxy-D-glucose positron emission tomography correlates with bactericidal activity of tuberculosis drug treatment. Antimicrob Agents Chemother **53:**4879–4884. http://dx.doi.org/10.1128/AAC.00789-09.
22. **Harper J, Skerry C, Davis SL, Tasneen R, Weir M, Kramnik I, Bishai WR, Pomper MG, Nuermberger EL, Jain SK.** 2012. Mouse model of necrotic tuberculosis granulomas develops hypoxic lesions. J Infect Dis **205:**595–602. http://dx.doi.org/10.1093/infdis/jir786.
23. **Driver ER, Ryan GJ, Hoff DR, Irwin SM, Basaraba RJ, Kramnik I, Lenaerts AJ.** 2012. Evaluation of a mouse model of necrotic granuloma formation using C3HeB/FeJ mice for testing of drugs against Mycobacterium tuberculosis. Antimicrob Agents Chemother **56:**3181–3195. http://dx.doi.org/10.1128/AAC.00217-12.
24. **Lanoix JP, Lenaerts AJ, Nuermberger EL.** 2015. Heterogeneous disease progression and treatment response in a C3HeB/FeJ mouse model of tuberculosis. Dis Model Mech **8:**603–610. http://dx.doi.org/10.1242/dmm.019513.
25. **Lanoix J-P, Ormond A, Dartois V, Nuermberger E.** 2014. Anti-tuberculosis activity of pyrazinamide varies by lesion type in C3HeB/FeJ mice, abstr 12. International Workshop on the Clinical Pharmacology of Tuberculosis Drugs. 5 September 2014, Washington, DC.
26. **Lanoix J-P, Ormond A, Dartois V, Nuermberger E.** 2014. Anti-tuberculosis activity of pyrazinamide varies by lesion type in C3HeB/FeJ mice, abstr A-20. Abstr Intersci Conf Antimicrob Agents Chemother. 5 to 9 September 2014, Washington, DC.
27. **Klinkenberg LG, Lee JH, Bishai WR, Karakousis PC.** 2010. The stringent response is required for full virulence of Mycobacterium tuberculosis in guinea pigs. J Infect Dis **202:**1397–1404. http://dx.doi.org/10.1086/656524.
28. **Larsen MH, Biermann K, Tandberg S, Hsu T, Jacobs WR.** 2007. Genetic manipulation of Mycobacterium tuberculosis. Curr Protoc Microbiol **Chapter 10:**Unit 10A.2. http://dx.doi.org/10.1002/9780471729259.mc10a02s6.
29. **Ioerger TR, Feng Y, Ganesula K, Chen X, Dobos KM, Fortune S, Jacobs WR, Mizrahi V, Parish T, Rubin E, Sassetti C, Sacchettini JC.** 2010. Variation among genome sequences of H37Rv strains of Mycobacterium tuberculosis from multiple laboratories. J Bacteriol **192:**3645–3653. http://dx.doi.org/10.1128/JB.00166-10.
30. **Via LE, Savic R, Weiner DM, Zimmerman MD, Prideaux B, Irwin SM, Lyon E, O'Brien P, Gopal P, Eum S, Lee M, Lanoix JP, Dutta NK, Shim T, Cho JS, Kim W, Karakousis PC, Lenaerts A, Nuermberger E, Barry CE III, Dartois V.** 2015. Host-mediated bioactivation of pyrazinamide: implications for efficacy, resistance, and therapeutic alternatives. ACS Infect Dis **1:**203–214. http://dx.doi.org/10.1021/id500028m.
31. **Miotto P, Cabibbe AM, Feuerriegel S, Casali N, Drobniewski F, Rodionova Y, Bakonyte D, Stakenas P, Pimkina E, Augustynowicz-Kopeć E, Degano M, Ambrosi A, Hoffner S, Mansjö M, Werngren J, Rüsch-Gerdes S, Niemann S, Cirillo DM.** 2014. Mycobacterium tuberculosis pyrazinamide resistance determinants: a multicenter study. mBio **5:**e01819–01814. http://dx.doi.org/10.1128/mBio.01819-14.
32. **Donald PR, Maritz JS, Diacon AH.** 2012. Pyrazinamide pharmacokinetics and efficacy in adults and children. Tuberculosis **92:**1–8. http://dx.doi.org/10.1016/j.tube.2011.05.006.
33. **Kjellsson MC, Via LE, Goh A, Weiner D, Low KM, Kern S, Pillai G, Barry CE, Dartois V.** 2012. Pharmacokinetic evaluation of the penetration of antituberculosis agents in rabbit pulmonary lesions. Antimicrob Agents Chemother **56:**446–457. http://dx.doi.org/10.1128/AAC.05208-11.
34. **Dartois V.** 2014. The path of anti-tuberculosis drugs: from blood to lesions to mycobacterial cells. Nat Rev Microbiol **12:**159–167. http://dx.doi.org/10.1038/nrmicro3200.
35. **Prideaux B, Via LE, Zimmerman MD, Eum S, Sarathy J, O'Brien P, Chen C, Kaya F, Weiner DM, Chen PY, Song T, Lee M, Shim TS, Cho JS, Kim W, Cho SN, Olivier KN, Barry CE, Dartois V.** 2015. The association between sterilizing activity and drug distribution into tuberculosis lesions. Nat Med **21:**1223–1227. http://dx.doi.org/10.1038/nm.3937.
36. **Kiem S, Schentag JJ.** 2008. Interpretation of antibiotic concentration ratios measured in epithelial lining fluid. Antimicrob Agents Chemother **52:**24–36. http://dx.doi.org/10.1128/AAC.00133-06.
37. **Ahmad Z, Fraig MM, Bisson GP, Nuermberger EL, Grosset JH, Karakousis PC.** 2011. Dose-dependent activity of pyrazinamide in animal models of intracellular and extracellular tuberculosis infections. Antimicrob Agents Chemother **55:**1527–1532. http://dx.doi.org/10.1128/AAC.01524-10.
38. **Schaible UE, Sturgill-Koszycki S, Schlesinger PH, Russell DG.** 1998. Cytokine activation leads to acidification and increases maturation of Mycobacterium avium-containing phagosomes in murine macrophages. J Immunol **160:**1290–1296.
39. **Jayaraman S, Song Y, Verkman AS.** 2001. Airway surface liquid pH in well-differentiated airway epithelial cell cultures and mouse trachea. Am J Physiol Cell Physiol **281:**C1504–C1511.
40. **Bodem CR, Lampton LM, Miller DP, Tarka EF, Everett ED.** 1983. Endobronchial pH. Relevance of aminoglycoside activity in gram-negative bacillary pneumonia. Am Rev Respir Dis **127:**39–41.
41. **Weiss C, Tabachnick J, Cohen HP.** 1954. Mechanism of softening of tubercles. III. Hydrolysis of protein and nucleic acid during anaerobic autolysis of normal and tuberculous lung tissue in vitro. AMA Arch Pathol **57:**179–193.
42. **Weiser OL, Dye WE.** 1956. Assay of Streptomycin in resected lung tissue. Conference on the chemotherapy of tuberculosis **12:**198–201.
43. **Fox W.** 1981. Whither short-course chemotherapy? Br J Dis Chest **75:**331–357. http://dx.doi.org/10.1016/0007-0971(81)90022-X.
44. **Mitchison DA.** 2000. Role of individual drugs in the chemotherapy of tuberculosis. Int J Tuberc Lung Dis **4:**796–806.
45. **Aono A, Chikamatsu K, Yamada H, Kato T, Mitarai S.** 2014. Association between pncA gene mutations, pyrazinamidase activity, and pyrazinamide susceptibility testing in Mycobacterium tuberculosis. Antimicrob Agents Chemother **58:**4928–4930. http://dx.doi.org/10.1128/AAC.02394-14.
46. **Timm J, Kurepina N, Kreiswirth BN, Post FA, Walther GB, Wainwright HC, Bekker LG, Kaplan G, McKinney JD.** 2006. A multidrug-resistant, acr1-deficient clinical isolate of Mycobacterium tuberculosis is unimpaired for replication in macrophages. J Infect Dis **193:**1703–1710. http://dx.doi.org/10.1086/504526.
47. **Tan S, Sukumar N, Abramovitch RB, Parish T, Russell DG.** 2013. Mycobacterium tuberculosis responds to chloride and pH as synergistic cues to the immune status of its host cell. PLoS Pathog **9:**e1003282. http://dx.doi.org/10.1371/journal.ppat.1003282.
48. **Irwin SM, Gruppo V, Brooks E, Gilliland J, Scherman M, Reichlen MJ, Leistikow R, Kramnik I, Nuermberger EL, Voskuil MI, Lenaerts AJ.** 2014. Limited activity of clofazimine as a single drug in a mouse model of tuberculosis exhibiting caseous necrotic granulomas. Antimicrob Agents Chemother **58:**4026–4034. http://dx.doi.org/10.1128/AAC.02565-14.